



Differential default mode network trajectories in asymptomatic individuals at risk for Alzheimer's disease

Patrizia A Chiesa, Enrica Cavedo, Andrea Vergallo, Simone Lista, Marie-Claude Potier, Marie-Odile Habert, Marion Dubois, Michel Thiebaut de Schotten, Harald Hampel, Hovagim Bakardjian, et al.

► To cite this version:

Patrizia A Chiesa, Enrica Cavedo, Andrea Vergallo, Simone Lista, Marie-Claude Potier, et al.. Differential default mode network trajectories in asymptomatic individuals at risk for Alzheimer's disease. *Alzheimer's & Dementia: Diagnosis, Assessment & Disease Monitoring*, 2019, 15 (7), pp.940-950. 10.1016/j.jalz.2019.03.006 . hal-02368904

HAL Id: hal-02368904

<https://hal.science/hal-02368904>

Submitted on 25 Oct 2021

HAL is a multi-disciplinary open access archive for the deposit and dissemination of scientific research documents, whether they are published or not. The documents may come from teaching and research institutions in France or abroad, or from public or private research centers.

L'archive ouverte pluridisciplinaire **HAL**, est destinée au dépôt et à la diffusion de documents scientifiques de niveau recherche, publiés ou non, émanant des établissements d'enseignement et de recherche français ou étrangers, des laboratoires publics ou privés.



Distributed under a Creative Commons Attribution - NonCommercial 4.0 International License

Differential default mode network trajectories in asymptomatic individuals at risk for Alzheimer's disease

Patrizia A. Chiesa^{a, b, c, d, *}

po.chiesa@gmail.com

Enrica Cavedo^{a, b, c, d}

Andrea Vergallo^{a, b, c, d}

Simone Lista^{a, b, c, d}

Marie-Claude Potier^d

Marie-Odile Habert^{a, b, c, d, e, f, g}

Bruno Dubois^{a, b, c, d, e, f, g}

Michel Thiebaut de Schotten^{a, b, c, d, e, f, g, h, i, j, k, l, m, n, o, p, q, r, s, t, u, v, w, x, y, z, 1, 2, 3, 4, 5, 6, 7, 8, 9, 10, 11, 12, 13, 14, 15, 16, 17, 18, 19, 20, 21, 22, 23, 24, 25, 26, 27, 28, 29, 30, 31, 32, 33, 34, 35, 36, 37, 38, 39, 40, 41, 42, 43, 44, 45, 46, 47, 48, 49, 50, 51, 52, 53, 54, 55, 56, 57, 58, 59, 60, 61, 62, 63, 64, 65, 66, 67, 68, 69, 70, 71, 72, 73, 74, 75, 76, 77, 78, 79, 80, 81, 82, 83, 84, 85, 86, 87, 88, 89, 90, 91, 92, 93, 94, 95, 96, 97, 98, 99, 100, 101, 102, 103, 104, 105, 106, 107, 108, 109, 110, 111, 112, 113, 114, 115, 116, 117, 118, 119, 120, 121, 122, 123, 124, 125, 126, 127, 128, 129, 130, 131, 132, 133, 134, 135, 136, 137, 138, 139, 140, 141, 142, 143, 144, 145, 146, 147, 148, 149, 150, 151, 152, 153, 154, 155, 156, 157, 158, 159, 160, 161, 162, 163, 164, 165, 166, 167, 168, 169, 170, 171, 172, 173, 174, 175, 176, 177, 178, 179, 180, 181, 182, 183, 184, 185, 186, 187, 188, 189, 190, 191, 192, 193, 194, 195, 196, 197, 198, 199, 200, 201, 202, 203, 204, 205, 206, 207, 208, 209, 210, 211, 212, 213, 214, 215, 216, 217, 218, 219, 220, 221, 222, 223, 224, 225, 226, 227, 228, 229, 230, 231, 232, 233, 234, 235, 236, 237, 238, 239, 240, 241, 242, 243, 244, 245, 246, 247, 248, 249, 250, 251, 252, 253, 254, 255, 256, 257, 258, 259, 260, 261, 262, 263, 264, 265, 266, 267, 268, 269, 270, 271, 272, 273, 274, 275, 276, 277, 278, 279, 280, 281, 282, 283, 284, 285, 286, 287, 288, 289, 290, 291, 292, 293, 294, 295, 296, 297, 298, 299, 300, 301, 302, 303, 304, 305, 306, 307, 308, 309, 310, 311, 312, 313, 314, 315, 316, 317, 318, 319, 320, 321, 322, 323, 324, 325, 326, 327, 328, 329, 330, 331, 332, 333, 334, 335, 336, 337, 338, 339, 340, 341, 342, 343, 344, 345, 346, 347, 348, 349, 350, 351, 352, 353, 354, 355, 356, 357, 358, 359, 360, 361, 362, 363, 364, 365, 366, 367, 368, 369, 370, 371, 372, 373, 374, 375, 376, 377, 378, 379, 380, 381, 382, 383, 384, 385, 386, 387, 388, 389, 390, 391, 392, 393, 394, 395, 396, 397, 398, 399, 400, 401, 402, 403, 404, 405, 406, 407, 408, 409, 410, 411, 412, 413, 414, 415, 416, 417, 418, 419, 420, 421, 422, 423, 424, 425, 426, 427, 428, 429, 430, 431, 432, 433, 434, 435, 436, 437, 438, 439, 440, 441, 442, 443, 444, 445, 446, 447, 448, 449, 450, 451, 452, 453, 454, 455, 456, 457, 458, 459, 460, 461, 462, 463, 464, 465, 466, 467, 468, 469, 470, 471, 472, 473, 474, 475, 476, 477, 478, 479, 480, 481, 482, 483, 484, 485, 486, 487, 488, 489, 490, 491, 492, 493, 494, 495, 496, 497, 498, 499, 500, 501, 502, 503, 504, 505, 506, 507, 508, 509, 510, 511, 512, 513, 514, 515, 516, 517, 518, 519, 520, 521, 522, 523, 524, 525, 526, 527, 528, 529, 530, 531, 532, 533, 534, 535, 536, 537, 538, 539, 540, 541, 542, 543, 544, 545, 546, 547, 548, 549, 550, 551, 552, 553, 554, 555, 556, 557, 558, 559, 560, 561, 562, 563, 564, 565, 566, 567, 568, 569, 570, 571, 572, 573, 574, 575, 576, 577, 578, 579, 580, 581, 582, 583, 584, 585, 586, 587, 588, 589, 590, 591, 592, 593, 594, 595, 596, 597, 598, 599, 600, 601, 602, 603, 604, 605, 606, 607, 608, 609, 610, 611, 612, 613, 614, 615, 616, 617, 618, 619, 620, 621, 622, 623, 624, 625, 626, 627, 628, 629, 630, 631, 632, 633, 634, 635, 636, 637, 638, 639, 640, 641, 642, 643, 644, 645, 646, 647, 648, 649, 650, 651, 652, 653, 654, 655, 656, 657, 658, 659, 660, 661, 662, 663, 664, 665, 666, 667, 668, 669, 670, 671, 672, 673, 674, 675, 676, 677, 678, 679, 680, 681, 682, 683, 684, 685, 686, 687, 688, 689, 690, 691, 692, 693, 694, 695, 696, 697, 698, 699, 700, 701, 702, 703, 704, 705, 706, 707, 708, 709, 710, 711, 712, 713, 714, 715, 716, 717, 718, 719, 720, 721, 722, 723, 724, 725, 726, 727, 728, 729, 730, 731, 732, 733, 734, 735, 736, 737, 738, 739, 740, 741, 742, 743, 744, 745, 746, 747, 748, 749, 750, 751, 752, 753, 754, 755, 756, 757, 758, 759, 760, 761, 762, 763, 764, 765, 766, 767, 768, 769, 770, 771, 772, 773, 774, 775, 776, 777, 778, 779, 780, 781, 782, 783, 784, 785, 786, 787, 788, 789, 790, 791, 792, 793, 794, 795, 796, 797, 798, 799, 800, 801, 802, 803, 804, 805, 806, 807, 808, 809, 810, 811, 812, 813, 814, 815, 816, 817, 818, 819, 820, 821, 822, 823, 824, 825, 826, 827, 828, 829, 830, 831, 832, 833, 834, 835, 836, 837, 838, 839, 840, 841, 842, 843, 844, 845, 846, 847, 848, 849, 850, 851, 852, 853, 854, 855, 856, 857, 858, 859, 860, 861, 862, 863, 864, 865, 866, 867, 868, 869, 870, 871, 872, 873, 874, 875, 876, 877, 878, 879, 880, 881, 882, 883, 884, 885, 886, 887, 888, 889, 890, 891, 892, 893, 894, 895, 896, 897, 898, 899, 900, 901, 902, 903, 904, 905, 906, 907, 908, 909, 910, 911, 912, 913, 914, 915, 916, 917, 918, 919, 920, 921, 922, 923, 924, 925, 926, 927, 928, 929, 930, 931, 932, 933, 934, 935, 936, 937, 938, 939, 940, 941, 942, 943, 944, 945, 946, 947, 948, 949, 950, 951, 952, 953, 954, 955, 956, 957, 958, 959, 960, 961, 962, 963, 964, 965, 966, 967, 968, 969, 970, 971, 972, 973, 974, 975, 976, 977, 978, 979, 980, 981, 982, 983, 984, 985, 986, 987, 988, 989, 990, 991, 992, 993, 994, 995, 996, 997, 998, 999, 1000}

Harald Hampel^{a, b, c, d, 1}

and the ► INSIGHT-preAD study group**

C. Audrain; A. Auffret; H. Bakardjian; F. Baldacci; B. Batrancourt; I. Benakki; H. Benali; H. Bertin; A. Bertrand; L. Boukadida; F. Cacciamani; V. Causse; E. Cavedo; S. Cherif Touil; P.A. Chiesa; O. Colliot; G. Dalla Barba; M. Depaulis; A. Dos Santos; B. Dubois; M. Dubois; S. Epelbaum; B. Fontaine; F. Francisque; G. Gagliardi; A. Genin; R. Genthon; P. Glasman; F. Gombert; M.O. Habert; H. Hampel; H. Hewa; M. Houot; N. Jungalee; A. Kas; M. Kilani; V. La Corte; F. Le Roy; S. Lehericy; C. Letondor; M. Levy; S. Lista; M. Lowrey; J. Ly; O. Makiese; I. Masetti; A. Mendes; C. Metzinger; A. Michon; F. Mochel; R. Nait Arab; F. Nyasse; C. Perrin; F. Poirier; C. Poisson; M.C. Potier; S. Ratovohery; M. Revillon; K. Rojkova; K. Santos-Andrade; R. Schindler; M.C. Servera; L. Seux; V. Simon; D. Skovronsky; M. Thiebaut de Schotten; O. Uspenskaya; M. Vlaincu

for the ► Alzheimer Precision Medicine Initiative (APMI) *(Please consider that the listed authors wrote the article on Behalf of the "Alzheimer Precision Medicine Initiative (APMI)" and the group therefore, should not be credited with the authorship of the article)*

Lisi Flores Aguilar; Claudio Babiloni; Filippo Baldacci; Norbert Benda; Keith L. Black; Arun L.W. Bokde; Ubaldo Bonuccelli; Karl Broich; Francesco Cacciola; Juan Castrillo; Enrica Cavedo; Roberto Ceravolo; Patrizia A. Chiesa; Olivier Colliot; Jean-Christophe Corvol; Augusto Claudio Cuello; Jeffrey L. Cummings; Herman Depypere; Bruno Dubois; Andrea Duggento; Stanley Durrleman; Valentina Escott-Price; Howard Federoff; Maria Teresa Ferretti; Massimo Fiandaca; Richard A. Frank; Francesco Garaci; Hugo Geerts; Remy Genthon; Nathalie George; Filippo S. Giorgi; Manuela Graziani; Marion Haberkamp; Marie-Odile Habert; Harald Hampel; Karl Herholz; Eric Karran; Seung H. Kim; Yosef Koronyo; Maya Koronyo-Hamaoui; Foudil Lamari; Todd Langevin; Stéphane Lehericy; Simone Lista; Jean Lorenceau; Dalila Mango; Mark Mapstone; Christian Neri; Robert Nisticò; Sid E. O'Bryant; Giovanni Palermo; George Perry; Craig Ritchie; Simone Rossi; Amira Saidi; Emiliano Santarnecchi; Lon S. Schneider; Olaf Sporns; Nicola Toschi; Steven R. Verdooner; Andrea Vergallo; Nicolas Villain; Lindsay A. Welikovitch; Janet Woodcock; Erfan Younesi

^aAXA Research Fund and Sorbonne University Chair, Paris, France

^bSorbonne University, GRC no 21, Alzheimer Precision Medicine (APM), AP-HP, Pitié-Salpêtrière Hospital, Boulevard de l'hôpital, Paris, France

^cBrain & Spine Institute (ICM), INSERM U 1127, CNRS UMR 7225, Boulevard de l'hôpital, Paris, France

^dDepartment of Neurology, Institute of Memory and Alzheimer's Disease (IM2A), Pitié-Salpêtrière Hospital, AP-HP, Boulevard de l'hôpital, Paris, France

^eICM Institut du Cerveau et de la Moelle épinière, CNRS UMR7225, INSERM U1127, UPMC, Hôpital de la Pitié-Salpêtrière, 47 Bd de l'Hôpital, Paris, France

^fLaboratoire d'Imagerie Biomédicale, Sorbonne Université, INSERM U 1146, CNRS UMR, Paris, France

^gDepartment of Nuclear Medicine, AP-HP, HôpitalPitié-Salpêtrière, Paris, France

^hCentre Acquisition et Traitement des Images (CATI, cati-neuroimaging.com), Paris, France

ⁱLaboratory of Alzheimer's Neuroimaging and Epidemiology, IRCCS Centro San Giovanni di Dio Fatebenefratelli, Brescia, Italy

ⁱⁱBrain Connectivity Behaviour Laboratory, Sorbonne Universities, Paris, France

ⁱⁱⁱGroupe d'Imagerie Neurofonctionnelle, Institut des Maladies Neurodégénératives-UMR 5293, CNRS, CEA University of Bordeaux, Bordeaux, France

*Corresponding author. Tel.: ~~+33 1 42 16 75 15/+33 1 57 27 44 81~~+33 (0)1 57 27 47 24; Fax: +33 (0)1 57 27 47 24.

¹These authors contributed equally to this study.

**The full list of members of the INSIGHT-preAD study group is reported in the Acknowledgment section.

~~AXA Research Fund and Sorbonne University Chair, Sorbonne University, GRC no 21, Alzheimer Precision Medicine (APM), ICM, INSERM U 1127, CNRS UMR 722, IM2A, Pitié-Salpêtrière Hospital.~~

~~Harald Hampel, MD, PhD, MA, MSc, SH.H is s~~peaker and coordinator of the Sorbonne Université Groupe de Recherche Clinique (GRC no. 21), “Alzheimer Precision Medicine (APM)”, Établissements Publics à caractère Scientifiqueet Technologique (E:P:S:T~~z~~), Alzheimer Precision Medicine Initiative (APMI) & Cholinergic System Working Group (CSWG).

~~Patrizia A. Chiesa, PhD, P.P.A.C. is a p~~ost-doctoral fellow AXA Research Fund & Sorbonne University Chair, Sorbonne University Department of Neurology, Institute of Memory and Alzheimer's Disease (IM2A), Brain & Spine Institute (ICM) François Lhermitte Building Pitié-Salpêtrière Hospital, ~~47 Boulevard de l'hôpital, 75651 Paris Cedex 13, France.~~^z Sorbonne University Clinical Research Group (GRC no. 21) “Alzheimer Precision Medicine (APM)” Établissements Publics à caractère Scientifique et Technologique (E:P:S:T~~z~~).^z Alzheimer Precision Medicine Initiative (APMI).

Abstract

Introduction

The longitudinal trajectories of functional brain dynamics and the impact of genetic risk factors in individuals at risk for Alzheimer's disease are poorly understood.

Methods

In a large-scale monocentric cohort of 224 amyloid stratified individuals at risk for Alzheimer's disease, default mode network (DMN) resting state functional connectivity (FC) was investigated between two serial time points across 2 years.

Results

Widespread DMN FC changes were shown in frontal and posterior areas, as well as in the right hippocampus. There were no cross-sectional differences, however, apolipoprotein E ε4 (*APOE* ε4) carriers demonstrated slower increase in FC in frontal lobes. There was no impact of individual brain amyloid load status.

Discussion

For the first time, we demonstrated that the pleiotropic biological effect of the *APOE* ε4 allele impacts the dynamic trajectory of the DMN during aging. Dynamic functional biomarkers may become useful surrogate outcomes for the development of preclinical targeted therapeutic interventions.

Keywords: Brain functional dynamics; ~~Longitudinal study;~~ Precision medicine; fMRI; Alzheimer's disease; Subjective memory complaints;~~APOE; Default mode network; Amyloid β~~

1 Background

Individuals at risk for complex, nonlinear dynamic diseases, such as Alzheimer's (AD), have active adaptive responses and compensatory mechanisms to maintain homeostasis ^[1]. ~~which results from the~~^zThese mechanisms are triggered and driven by an interplay between genetic/epigenetic and environmental factors. Stratifying individuals according to the genetic risk factors for AD is a crucial step to attain reliable measures essential for identifying distinctive endophenotypes. Breakthrough technological advances have facilitated synergistic research alliances between geneticists and neuroscientists to determine how genomic factors affect brain structure, function, and metabolism. Overall, robust evidence is mounting, indicating several genes associated with an increased risk of AD ^[2]. The *apolipoprotein E (APOE)* ε4 allele is considered the most relevant genetic risk factor for late-onset AD and is observed in up to 50% of all cases of sporadic AD ^[3]. *APOE* gene is involved in many different processes: it regulates amyloid β (Aβ) oligomerization, aggregation, and receptor-mediated clearance, brain lipid transport, glucose metabolism, neuronal signaling, and neuroinflammation ^[4–6]. In vivo pathophysiological or topographic biomarkers (e.g., reduced metabolism ^[7], hippocampal atrophy ^[8], and cortical thickness ^[9]) provide supportive evidence for the altering impact of the *APOE* ε4 allele on brain changes occurring across a continuum from physiological conditions to AD pathophysiology.

In the past decade, brain functional connectivity (FC) has become a promising candidate biomarker for early identification of brain functional changes related to AD pathophysiology ^[10]. Functional neuroimaging genetics offers an efficient strategy for characterizing intermediate phenotypes of AD and improving the understanding of genetic pathways that interact with brain functioning ^[11]. Although the field is relatively young, the number of studies investigating possible downstream effects of risk genes on brain

functional dynamics is rapidly growing. Particularly, *APOE* ε4 carriers show specific and consistent alterations in the default mode network (DMN) [12] connectivity at rest, including decreased connectivity in the middle and posterior regions, and increased connectivity in the frontal and lateral structures [13–21]. Increases in resting state FC (rsFC) at the early stages of AD have been interpreted as either upstream or downstream brain compensatory mechanisms between brain regions typically affected in AD [22], mostly in the DMN [23–25]. Whether different aging trajectories occur in the DMN in cognitively intact *APOE* ε4 carriers and noncarriers, however, is currently unknown and requires longitudinal investigations of the DMN at the individual level. This will be an essential step forward for the functional neuroimaging genetic field because, to date, studies have been almost exclusively conducted using cross-sectional designs, exploring DMN alterations over time by comparing cross-sectional groups with increased genetic risk across different severity stages [2].

Longitudinal methods are particularly sensitive in detecting individual functional changes in neural networks. LongitudinalLong-term follow-up studies performed on cognitively intact individuals at risk for AD individuals would enable clinical researchers to trace pathophysiological trajectories from health to late dementia stages and identify critical windows for failing compensatory mechanisms. This is of special interest for older individuals with subjective memory complaints (SMCs), a condition at increased risk of developing AD [26,27]. Such memory complaints may represent early signs of a wider cognitive impairment and be considered as a valid measure of self-reported memory decline [27]. Both memory complaints and the presence of at least one *APOE* ε4 allele predict cognitive decline at an early stage of AD [28]. However, no evidence of longitudinal alterations in functional networks has been established so far in asymptomatic individuals at risk for AD.

We compared longitudinal DMN resting state functional connectivity (rsFC) between two time points (24 months apart) in a large-scale standardized observational university expert center-based monocentric cohort of 224 cognitively intact individuals with SMC, devoid of any objective cognitive impairment. Given (1) the critical role of *APOE* in regulating Aβ-related processes [4], (2) the strong prevalence of the *APOE* ε4 allele in Aβ positive individuals across the spectrum of AD, and (3) the massive effect of brain amyloid on brain structural [22,29] and functional [22,30,31] connectivity, we evaluated the impact of the individual amyloid status on brain aging trajectories related to *APOE* ε4 status.

2 Materials and methods

2.1 Participants

Data used in the preparation of this article were obtained from the “INveStIGation of AlzHeimer’sPredicTors in Subjective Memory Complainers” (INSIGHT-preAD) study [detailed method is available in [24]]. The INSIGHT-preAD study includes 318 cognitively intact Caucasian older adults recruited from the community in the wider Paris area, France, aged 70 to 85 years, with SMC, defined as follows: (1) Participants answered “YES” to both questions “Are you complaining about your memory?” and “Is it a regular complaint that has lasted now more than 6 months?”; (2) participants present intact cognitive functions based on Mini-Mental State Examination (≥27), Clinical Dementia Rating scale (0), and Free and Cued Selective Rating Test (total score ≥41). Written informed consent was obtained from all participants. The study was approved by the local Institutional Review Board and has been conducted in accordance with the Helsinki Declaration of 1975.

For the present study, we had considered only participants who underwent the resting state functional magnetic resonance imaging (rs-fMRI) acquisition both at the first time point (M0) and after 24 months (M24). Demographic characteristics, cognitive performance, and *APOE* genotype of the final subset (224 participants) are shown in Table 1.

Table 1 Demographic characteristics, global cognitive performance, and APOE genotype of the final subset, including 224 cognitively intact individuals with SMC				
		All	APOE ε4 noncarriers	APOE ε4 carriers
Participants (female)		224 (133)	180 (107)	44 (26)
Education		6.3 ± 2.0	6.1 ± 2.1	6.4 ± 2.2
Age ± SD	M0	75.5 ± 3.4	75.5 ± 3.4	75.6 ± 3.5
	M24	77.5 ± 3.5	77.5 ± 3.5	77.6 ± 3.5
MMSE ± SD	M0	28.6 ± 1.0	28.6 ± 1.0	28.5 ± 1.0
	M24	28.8 ± 1.3	28.7 ± 1.4	28.8 ± 1.3

Abbreviations: APOE, apolipoprotein E; MMSE, Mini-Mental State Examination; SD, standard deviation; SMC, subjective memory complaint.

NOTE. Education was measured in a range from 1 (no diploma) to 8 (bachelor, master’s degree, or doctorate).

2.2 Clinical and neuropsychological assessments

A comprehensive neuropsychological battery was administered to all participants of the INSIGHT-preAD cohort to assess they were cognitively intact in all relevant cognitive domains [27].

2.3 APOE genotype

Participants were divided into two groups based on the *APOE* status: individuals carrying at least one *APOE* $\epsilon 4$ allele (genotype $\epsilon 4/\epsilon 4$ and $\epsilon 4/\epsilon 3$) were classified as *APOE* $\epsilon 4$ carriers (*APOE* $\epsilon 4+$); the others (genotype $\epsilon 2/\epsilon 2$, $\epsilon 2/\epsilon 3$, and $\epsilon 3/\epsilon 3$) were classified as *APOE* $\epsilon 4$ noncarriers (*APOE* $\epsilon 4-$) [detailed method is available in [24]].

2.4 Amyloid status definition

Reconstructed **PET**positron emission tomography images were analyzed with a pipeline developed by the **GATH**Centre Acquisition et Traitement des Images (CATI), a neuroimaging platform funded by the French Plan Alzheimer (<http://cati-neuroimaging.com>); detailed method is available in [24]].

Our cohort was divided into two subgroups based on their cortical **SUVR**standardized uptake value ratio value, that is, amyloid positive (Amy+) and amyloid negative (Amy-) individuals [32]. The **SUVR**standardized uptake value ratio threshold of 0.79 to determine abnormality uptake was extracted performing linear correlation between our method [32] and the method used by Besson et al. [33] using 53 **PET**positron emission tomography scans from another French study, the **IMAP**Imagerie Multimodale de la maladie de l'Alzheimer à un stade Précoce (IMAP) cohort (multimodal neuroimaging project on early Alzheimer's disease).

2.5 MRI acquisition and preprocessing

MRI images were acquired using a Siemens MagnetomVerio (Erlangen, Germany) 3-T scanner, equipped with a quadrature detection head coil with 12 channels (transmit-receive circularly polarized-head coil). Three-dimensional (3D) TurboFLASH sequences were performed (orientation sagittal; repetition time 2300 ms; echo time 2.98 ms; inversion time 900 ms; flip angle 9°; 176 slices; slice thickness 1 mm; field of view 256 × 240 mm; matrix 256 × 240; bandwidth 240 Hz/Px).

2.6 rs-fMRI acquisition and preprocessing

Both baseline and follow-up scanning were performed on a 3 T MRI scanner qualified by the central MRI analysis core at the Cogimage Team, ICM (Paris, France). During the rs-fMRI scan, participants were instructed to keep their eyes closed and stay as still as possible. The rs-fMRI images were collected by using an echo-planar imaging sequence (repetition time 2460 ms, echo time 30 ms, slice thickness 3 mm, matrix 64 × 64, voxel size 3 × 3 × 3 mm³, number of volumes 250, number of slices 45, run 1) sensitive to blood oxygenation level-dependent contrast (T2* weighting).

The rs-fMRI data were preprocessed using **BGB**the Brain Connectivity and Behaviour toolkit v4.0.0 (available at <http://toolkit.bcblab.com>) [34] based on **FSL**FMRIB Software Library (FSL) (available at <https://fsl.fmrib.ox.ac.uk>), which has previously been used successfully to identify the DMN [35]. Each participant's first 10 volumes were excluded to avoid potential noise related to the equilibrium of the magnet and participant's adaptation to the scanner. After individual correction for movement, the remaining 240 volumes were first motion corrected using **MCFLIRT**a motion-correction tool based on FMRIB's Linear Image Registration Tool, then corrected for slice timing, smoothed with a full half width maximum equal to 1.5 times the largest voxel dimension, and finally filtered for low temporal frequencies using a Gaussian-weighted local fit to a straight line. These steps are available in Feat as part of **FSL**FMRIB Software Library package. fMRI images are linearly registered to the T1 structural images. Estimated motion parameters, the first eigenvariate of the **WM**white matter and **GSF**cerebrospinal fluid and their first derivatives were regressed out from the functional data. We used masks based on the T1 derived three-class segmentation thresholded to a probability value of .9, registered to the rs-fMRI images and binarized. Finally, the first derivative of the motion parameters, **WM**white matter, and **GSF**cerebrospinal fluid signal was calculated by linear convolution between their time course and a [-1 0 1] vector.

Given that rs-fMRI signal can be severely affected by motion, ~~an independent component analysis (ICA)-AROMA-procedure was used to~~a strategy based on the independent component analysis for Automatic Removal of Motion Artifacts (ICA-AROMA) was used to estimate the signal fluctuation associated with motion and then to regress it out from the fMRI data [36]. ICA-AROMA performs an ICA decomposition of the data and estimates which components reflect motion-related noise in the fMRI signal on the basis of a robust set of spatial and temporal features because of the distinctiveness of the motion-related components [37]. This approach outperforms other methods, such as the regression of the motion parameter estimates, while limiting **at** the same time the loss in degrees of freedom [36]. Compared with spike removal methods such as scrubbing [38], ICA-AROMA has the advantage of preserving the temporal structure of the fMRI signal.

2.7 rs-fMRI independent component analysis

Analysis of the rs-fMRI data was carried out using probabilistic ICA as implemented in Multivariate Exploratory Linear Optimized Decomposition into Independent Components, part of FMRIB's Software Library. Multivariate Exploratory Linear Optimized Decomposition into Independent Components was used to decompose the original concatenated 4D rs-fMRI data set into different spatial and temporal components [39]. The preprocessed functional data for each participant were temporally concatenated into a single 4D data set, which was analyzed using ICA.

In this analysis, the data set was decomposed into 20 independent components. However, it should be noted that there is no consensus yet on how to choose the optimal number of components [40]. The dual regression analysis was performed to identify subject-specific time courses and spatial maps [41]. In the first step, the 20 components were used in a linear model fit against each individual subject's fMRI data set to create the average time course within each network for every subject (spatial regression), ultimately resulting in 20 z-score maps per individual per visit. In the second step, the personalized time courses were regressed back onto that participant's fMRI data set to create personal spatial maps (temporal regression). This gives 20 3D images per individual per visit, with voxelwise the z scores of FC to each of the templates.

The first step (group ICA) was performed using the first time point (M0) of all individuals. To keep the spatial patterns consistent across analyses, the resulting 20 independent components were used in the next dual regression steps to analyze the second data point (M24).

The DMN was finally selected by visual inspection based on the previous literature [42].

2.8 Statistical analyses

To perform longitudinal analyses, we calculated the change in rsFC (i.e., Δ FC) after 24 months (M24) as the change in rsFC from the first acquisition (M0).

The FSL's randomized permutation-testing tool (5000 permutations) was used to detect statistically significant differences within the DMN, correcting for age. Familywise error (FWE) correction for multiple comparisons was performed, implementing threshold-free cluster enhancement (TFCE) using a significance threshold of $P < .05$.

2.8.1 Effect of time

The resulting Δ FC values were compared with the null hypothesis of no change in DMN FC after 24 months by using one simple t test on Δ FC.

2.8.2 Effect of APOE

Given the pattern of results described in previous works [2], we were primarily interested in the comparison of *APOE* $\epsilon 4$ carriers (*APOE* $\epsilon 4+$) versus *APOE* $\epsilon 4$ noncarriers (*APOE* $\epsilon 4-$). Cross-sectional group differences between *APOE* $\epsilon 4+$ and *APOE* $\epsilon 4-$ participants were firstly identified using two sample t tests in FSL for M0. Then, we evaluated the longitudinal impact of being *APOE* $\epsilon 4+$ versus *APOE* $\epsilon 4-$, using a two independent t test on Δ FC.

2.8.3 Impact of the amyloid status

Finally, we investigated any potential effect of amyloid on the longitudinal brain dynamics changes. To this aim, a 2 (amyloid status, Amy+ vs. Amy-) \times 2 (*APOE* genetic risk, *APOE* $\epsilon 4+$ vs. *APOE* $\epsilon 4-$) repeated measure analysis of variance was performed in [FEATfMRI Expert Analysis Tool](#) (available at <https://fsl.fmrib.ox.ac.uk/fsl/wiki/FEAT>) on Δ FC. Results were corrected for multiple comparisons using correction for FWE rate and TFCE, which is similar to cluster-based thresholding, but generally more robust and without the identification of the arbitrary initial cluster-forming threshold. TFCE is recommended when randomization is performed [43].

3 Results

3.1 Participants

From the INSIGHT-preAD cohort, we included only 242 participants. See Fig. 1 for details.

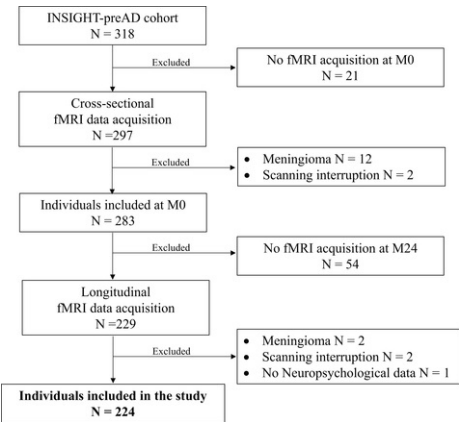


Fig. 1 Flow diagram shows participant inclusion process for the present study from the initial INSIGHT-preAD cohort. Abbreviation: fMRI, functional magnetic resonance imaging.

3.2 DMN extraction

After individual correction for movement, an ICA identified the group level DMN, as depicted in Fig. 1 of the [Supplemental Material](#) [Supplementary Material](#), where classical hubs can be seen, such as the Precuneus (Pcu), the inferior parietal lobe, the anterior and posterior cingulate cortices (ACC and PCC), as well as the medial frontal and prefrontal cortices [12]. Individual maps were subsequently extracted using a dual regression approach [41].

3.3 Main longitudinal effects

Fig. 2 illustrates rsFC longitudinal changes in the DMN for more than a time period of 24 months. The widespread increase in rsFC concerned the medial prefrontal, frontal, and posterior DMN regions, including the ACC extending to the anterior medial frontal cortex, the PCC, the Pcu, and the left hippocampus and parahippocampus (Fig. 2, green-red scale). Significant decrease in rsFC was minimal involving the most dorsal portion of the Pcu (Fig. 2, blue scale).

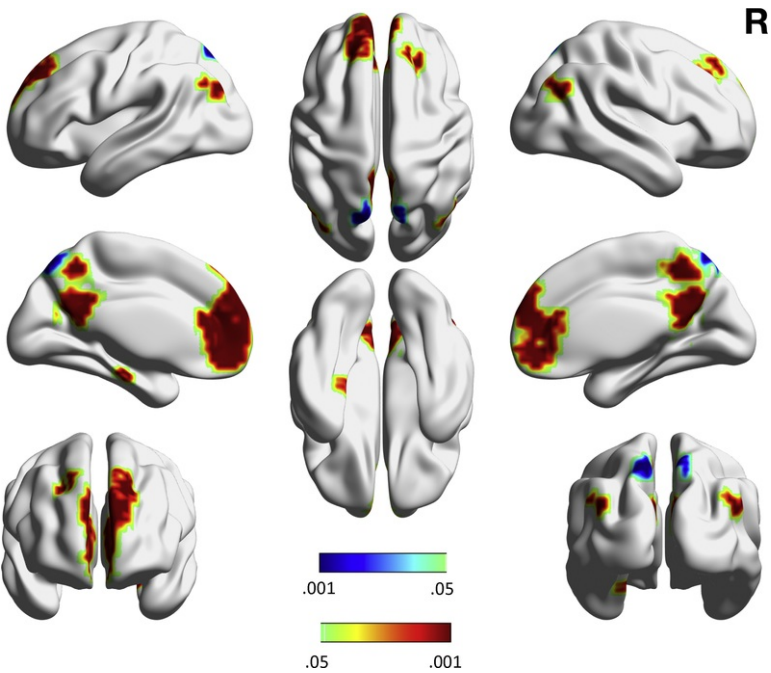


Fig. 2 DMN longitudinal changes in 224 participants for more than a time period of 24 months. Widespread increased (green-red voxels) DMN rsFC was found in our participants, including bilateral frontal and prefrontal regions, ACC, PCC, Pcu, angular gyrus, left hippocampus, and parahippocampus. Pcu also showed decreased rsFC in time (blue voxels). The statistical maps were thresholded using TFCE and $P < .05$ familywise error corrected, cluster >15 voxels. All results are described in [Table 2](#) with their coordinates in the [MNI](#) [Montreal Neurological Institute](#) space.

Brain region	BA	Voxels	<i>t</i> value	P_{FWE}	Peak		
					X (mm)	Y (mm)	Z (mm)
Increased connectivity	10	602	14.2	<.001	−2	62	20
	23	330	10.8	<.001	−6	−54	28
	39	48	9.53	<.001	50	−70	32
	39	32	9.15	<.001	−46	−70	36
	9	29	7.63	<.001	22	42	40
	30	16	6.25	<.001	−26	−22	−24
Decreased connectivity	7	61	8.36	<.001	−14	−74	56

Abbreviations: BA, Brodmann area; DMN, default mode network; FWE, familywise error.

3.4 APOE ε4 genotype effect

We asked the question whether carrying the *APOE* ε4 allele affected the DMN rsFC. First, we compared the rsFC at the initial time point (M0): cross-sectional comparisons between *APOE* ε4 carriers (*APOE* ε4+) and *APOE* ε4 noncarriers (*APOE* ε4-) revealed that the presence of the ε4 allele did not significantly modulate the DMN rsFC. Second, we assessed the genetic impact of the *APOE* ε4 allele on the rate of individual aging of the DMN rsFC: the longitudinal analysis indicated that individuals carrying the ε4 allele presented a slower increase in rsFC in the frontal lobes ($P < .05$ TFCE corrected), specifically in BA9, BA10, BA46, bilaterally (Fig. 3). Hence, although the level of FC between *APOE* ε4+ and *APOE* ε4- is comparable, the rate of increase in FC in *APOE* ε4+ is significantly slower than *APOE* ε4-.

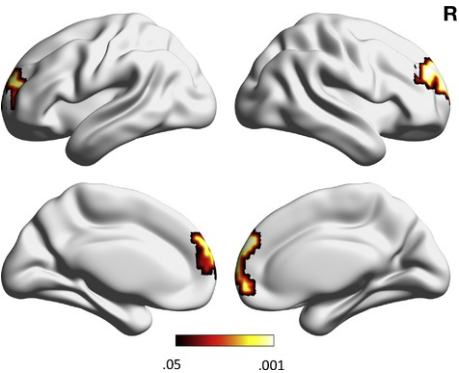


Fig. 3 Effect of *APOE* on the longitudinal DMN changes. The comparison of the DMN changes over time between *APOE* ε4- and *APOE* ε4+ showed a significant increased rsFC in the frontal and prefrontal areas over time [245 voxels, [30 50 28], $P_{FWE} < .001$]. No effects of global amyloid load or an interaction effect between the amyloid status and *APOE* were found. The statistical maps were thresholded using TFCE and $P < .05$ familywise error corrected.

3.5 Impact of amyloid status on functional dynamics of the APOE ε4 genotype

Whether individuals' amyloid status may further influence connectivity dynamics changes linked to the presence of *APOE* ε4 allele is still unknown. Therefore, we perform a 2×2 repeated measures analysis of variance to evaluate the presence of an interaction effect between *APOE* and amyloid status. Results showed that neither the amyloid nor the *APOE* × amyloid interaction were significant on the longitudinal changes ($P < .05$ FWE corrected).

4 Discussion

In summary, brain network dynamics were examined in a standardized large-scale, observational monocentric university expert center cohort of 224 cognitively intact individuals with SMC, devoid of any objective cognitive impairment. Consistent with our a priori hypothesis, rsFC changes within the DMN were found 2 years after the first rs-fMRI evaluation. In addition, we provided in vivo evidence that the *APOE* ε4 genotype leads to different distinct DMN functional alterations regardless of the individual amyloid status.

At the group level, DMN changes were particularly evident in the posterior, frontal, and prefrontal cortices, as well as in the right hippocampus. Consistently with previous findings [44–47], there might have been a reorganization of brain rsFC induced by age-related mechanisms and/or disease progression. The increased brain activity during aging and at early stages of AD may serve as a compensatory mechanism and may reflect the enhanced metabolic demand engaged by an adaptive brain to cope with disruptive signals affecting specific vulnerable neural regions. This increased compensatory resilient response has frequently been observed in the frontal lobes [48,49], which may play a key role for cognitive reserve [50]. Overall, in our population, compensatory mechanisms seem to involve a posterior-anterior shift [51], which is characterized by reduced activation in the posterior midline cortex along with increased activity in medial frontal cortex [48,49]. Consistent with this model, we found decreased rsFC in the most dorsal part of the Pcu. However, we also showed the presence of increased activity in the more ventral Pcu extending to the PCC. The presence of different distinct expression of posterior alterations might originate from differentmany sources. First, owing to the functional heterogeneity of the Pcu [52,53], each subregion might be differently damaged at the early stages of AD. Here, we found decreased rsFC in the dorsal Pcu, which showed positive rsFC with the superior parietal cortex, and negative rsFC with the orbital and frontal cortices, the amygdala, and the cerebellum [52]. Additional functional studies are needed to clarify whether specific Pcu subregions are differently affected across the whole AD continuum. Second, rsFC might start decreasing in a narrow subregion of the Pcu and slowly perturbing other adjacent neurons before spreading the functional impairment to the rest of the brain through a mechanism of diaschisis [54]. We hypothesize that spatiotemporal changes across brain networks, in the context of complex and nonlinear dynamic diseases such as AD, may have a stepwise evolution from an “intra-network phase” to a whole-network and, ultimately, a multinetwork compensation phase. Spreading of pathophysiological processes during brain disease phases are mediated by complex mechanisms [54], which are not fully understood yet. However, two longitudinal data points are insufficient to investigate the potential spreading of the functional impairment in time. Future longitudinal data-follow-up acquisitions of the INSIGHT-preAD cohort may provide us with key evidence in this regard. In the incoming future, advanced The implementation of multimodal approaches, such as neuroimaging genetics integrated with the implementation of computational biologychemical analyses, will provide the basis to establish whether the trajectories of molecular/cellular

pathways are linked to dynamic patterns of neural network reorganization~~in our population~~, thus potentially ~~mapping~~~~classifying~~ compensatory or adaptive strategies.

We ~~may~~~~can~~ argue that methodological choices may also have affected the results. For instance, although SMC represents per se a condition at risk of developing AD [26,28], the different endophenotypes included in such heterogeneous group may range from physiological brain aging to AD-related signatures (i.e., preclinical AD). Moreover, although the application of ICA in rs-fMRI studies is a powerful analytic method to separate bold signal from physiological noise induced by the cardiac pulse and respiration, some residual noise might still be present in the components [55]. Finally, we focused our attention on the DMN; however, early dysfunctions may involve further large-scale networks [56]. More complex methods~~s~~ will allow us to extend the analyses to all the brain networks that are normally affected in neurologic disorders, including AD. Finally, it is worth to note that the INSIGHT-preAD cohort includes well-educated individuals, which may be able to compensate more effectively. As a consequence, our cohort may be affected by a selection bias that comes from errors in selecting the study participants and/or from factors affecting the study participation.

Successively, the impact of the *APOE* ϵ 4 genotype was investigated. In the present study, no significant results were found between *APOE* ϵ 4~~-~~ and *APOE* ϵ 4+ at ~~the first time point~~~~the first time point~~ (M0). The reason why cross-sectional findings on the DMN connectivity do not consistently demonstrate differences between *APOE* ϵ 4~~-~~ and *APOE* ϵ 4+ is still debated in the literature [2]. It has been previously shown that the inclusion of a wide age range in the same sample generated conflicting results: both decreased [13] and increased [14,15] connectivity were found cross-sectionally in a number of DMN nodes. In this regard, Staffaroni et al. [21] did not find any significant difference between *APOE* ϵ 4+ and *APOE* ϵ 4~~-~~ ~~in~~at baseline or ~~in the~~ longitudinal trajectory of DMN rsFC by including individuals at different aging stages (ages 49–87 years~~}, with only 23 older adults.~~). Our data might be similarly affected by the inclusion of different endophenotypes whose differences are exacerbated later in time. It has been also demonstrated that different neural dynamics are detectable in mutation carriers of several additional genes, such as phosphatidylinositol binding clathrin assembly protein (PICALM), clusterin (CLU), and bridging integrator 1 (BIN1) genes across the lifespan [2]. Liu et al. [57] showed that the outer mitochondria membrane 40 homolog (TOMM40) genotype may modulate regional spontaneous brain activity and is related to the progression of individuals in prodromal phase of AD. Several additional pathophysiological mechanisms, epigenetic factors, and interactions with other genes might need to be considered and integrated in future studies.

For the first time, we demonstrated in vivo evidence that carrying the *APOE* ϵ 4 allele leads to a different aging trajectory of DMN. According to our results, we suggest that carrying the *APOE* ϵ 4 allele leads to different longitudinal changes: *APOE* ϵ 4+ showed a slower increase in rsFC in the frontal and prefrontal areas compared with *APOE* ϵ 4~~-~~. Future studies including neuropsychological outcome measures will disclose whether such dynamics represent compensatory mechanisms to cope with pathophysiological processes driven by *APOE* ϵ 4 genotype.

Given the established association between *APOE* ϵ 4 genotype and the impairment of A β metabolism with subsequent extracellular accumulation [58], we further investigated whether the functional changes related to *APOE* ϵ 4 might be partially explained by the presence of increased fibrillary A β deposition. Our data suggest that *APOE* ϵ 4 leads to DMN rsFC changes regardless of the A β brain accumulation, indicating that other biological mechanisms, besides A β , are driven by the *APOE* ϵ 4 allele. Such finding is in line with both animal and human studies reporting a pleiotropic effect of *APOE* ϵ 4 on several molecular pathways, including, among others, tau hyperphosphorylation, inhibition of neurite outgrowth, and axonal sprouting.

Interestingly, a recent study showed that brain A β deposition seems to be associated with specific network dysfunction even in the absence of neural hypometabolism [59]. However, individuals were not genotyped for *APOE*, thus leading to potential ambiguous results. Given that *APOE* ϵ 4 has a powerful effect on cerebral A β metabolism [58], the presence of neural dysfunctions may be linked to the *APOE* ϵ 4 allele, which downstream promotes A β deposition. Consequently, the DMN dysfunction might be a cause, rather than a consequence, of A β aberrant pathways [60]. It has been previously shown that the neuronal components of the DMN have an increased vulnerability to bioenergetic failure because of their highly persistent activation [61]. Thus, a reorganizational pattern of connectivity within the DMN may ensure adaptation for bioenergetic cellular stress.

The dramatic rate of failures of large-scale clinical trials has suggested that novel target and outcome measures are needed to overcome insufficient~~clinical trials~~ ~~design~~ [62–64]. The new challenge in pharmacologic Research and Development programs is to reconsider previous traditional hypotheses and to better define how preclinical data can support novel data-driven hypotheses, how to perform a convincing and evidence-driven “preclinical to clinical” translation, how to ~~longitudinally~~ chart the biological effect of a candidate drug ~~over time during investigation~~, and~~,~~ finally~~,~~ how to assess whether such a biological effect is ~~really~~ ~~truly~~ correlated with functional and ~~later~~ clinical improvement.

Connectomics within the DMN have increasingly been recognized as established biomarkers for several contexts of use even in preclinical stages of the disease [10,47,65,66]. Alterations in connectivity, which extend beyond the DMN [18], are expected to be designated as further promising biomarker candidates or even as much needed surrogate biomarker candidates for clinical outcome [67]. Novel technologies and sophisticated computational analyses will soon enable integrating clinical, genetic/epigenetic, and neurodynamic/neuroimaging data, providing a full individual biological makeup. Biomarker-guided predictive trajectories will further permit researchers to identify and stratify preclinical biologically defined “at risk” populations. ~~The~~A new conceptual paradigm ~~of~~~~—~~precision medicine~~—~~~~operates~~~~ing~~ in this context ~~and~~ aims at tailoring medical treatments to the individual genetic drivers, pathophysiological, and clinical characteristics of the disease for the single patient [63]. In this perspective, the future precision medicine will ensure the successful achievement of innovative personalized therapeutic strategies to prevent, halt, and cure AD and other complex neurodegenerative diseases.

Research in Context

1. Systematic review: We reviewed the literature using traditional (e.g., PubMed) sources and meeting abstracts and presentations. Although the longitudinal brain functional trajectories of Alzheimer's disease (AD) have not been studied yet, recent publications describing the cross-sectional aspects of the brain functional dynamics are appropriately cited.
2. Interpretation: Consistently with previous findings, there might have been a reorganization of brain functional connectivity induced by age-related mechanisms and/or disease pathophysiological progression. In addition, we demonstrated that the pleiotropic biological effect of the *APOE* ϵ 4 allele impacts the dynamic trajectory of the default

mode network over time

3. Future directions: These results may generate early and modifiable functional outcomes in the perspective of individualized and targeted therapeutic preclinical interventions. Further studies may evaluate (1) the functional changes in either physiological or pathophysiological conditions, such as AD, (2) the functional dynamics associated with conversion to AD, and (3) the inclusion of functional outcomes in clinical trials.

Acknowledgments

The study was promoted by INSERM in collaboration with ICM, IHU-A-ICM, and Pfizer and has received a support within the “Investissement d’Avenir” (ANR-10-AIHU-06). The study was promoted in collaboration with the “CHU de Bordeaux” (coordination CIC EC7), the promoter of Memento cohort, funded by the Foundation Plan-Alzheimer. The study was further supported by AVID/Lilly.

The research leading to these results was supported by the *Colam Initiatives* and the “*Fondation pour la Recherchesur Alzheimer*,” Paris, France.

This publication is within the framework of the Program “MIDAS” led by the Sorbonne University Foundation and sponsored by MSDAVENIR.

Michel Thiebaut de Schotten is supported by the “AgenceNationale de la Recherche” (grant number ANR-13- JSV4-0001-01) and a European Research Council Consolidator Investigator Award (ERC-2018-COG 818521).

H.H. is supported by the AXA Research Fund, the “Fondation partenariale Sorbonne Université” and the “Fondation pour la Recherchesur Alzheimer,” Paris, France. Ce travail a bénéficié d'une aide de l'Etat “Investissements d’avenir” ANR-10-IAIHU-06. The research leading to these results has received funding from the program “Investissements d’avenir” ANR-10-IAIHU-06 (Agence Nationale de la Recherche-10-IA Agence Institut Hospitalo-Universitaire-6).

Author contributions: P.A.C., E.C., B.D., H.H., and M.T.S. have contributed to the conception and design of the study. P.A.C., E.C., M.C.P., M.O.H., and M.T.S. have contributed to acquisition and analysis of data. P.A.C., A.V., E.C., S.L., M.T.S., and H.H. have contributed to drafting and revising a significant portion of the manuscript.

Competing financial interests: H.H. serves as a Senior Associate Editor for the Journal Alzheimer’s & Dementia; he received lecture fees from Biogen and Roche, research grants from Pfizer, Avid, and MSD Avenir (paid to the institution), travel funding from Functional Neuromodulation, Axovant, Eli Lilly and company, Takeda and Zinfandel, GE-Healthcare, and Oryzon Genomics, consultancy fees from [Qynapse](#), Jung Diagnostics, Cytox Ltd, Axovant, Anavex, Takeda and Zinfandel, GE Healthcare, and Oryzon Genomics, Functional Neuromodulation, and participated in scientific advisory boards of Functional Neuromodulation, Axovant, [Eisai](#), Eli Lilly and Company, Cytox Ltd, GE Healthcare, Takeda and Zinfandel, Oryzon Genomics, and Roche Diagnostics. H.H. is a coinventor in the following patents as a scientific expert and has received no royalties:

- In vitro multiparameter determination method for the diagnosis and early diagnosis of neurodegenerative disorders. Patent number: 8916388.
- In vitro procedure for diagnosis and early diagnosis of neurodegenerative diseases. Patent number: 8298784.
- Neurodegenerative markers for psychiatric conditions. Publication number: 20120196300.
- In vitro multiparameter determination method for the diagnosis and early diagnosis of neurodegenerative disorders. Publication number: 20100062463.
- In vitro method for the diagnosis and early diagnosis of neurodegenerative disorders. Publication number: 20100035286.
- In vitro procedure for diagnosis and early diagnosis of neurodegenerative diseases. Publication number: 20090263822.
- In vitro method for the diagnosis of neurodegenerative diseases. Patent number: 7547553.
- [GSFCerebrospinal fluid](#) diagnostic in vitro method for diagnosis of dementias and neuroinflammatory diseases. Publication number: 20080206797.
- In vitro method for the diagnosis of neurodegenerative diseases. Publication number: 20080199966.
- Neurodegenerative markers for psychiatric conditions. Publication number: 20080131921.

INSIGHT-preAD Study Group: [Audrain C, Auffret A, Bakardjian H, Baldacci F, Batrancourt B, Benakki I, Benali H, Bertin H, Bertrand A, Boukadida L, Gacciamani F, Causse V, Cavedo E, Cherif Touil S, Chiesa PA, Colliot O, Dalla Barba G, Depaulis M, Dos Santos A, Dubois B, Dubois M, Epelbaum S, Fontaine B, Francisque H, Gagliardi C, Genin A, Genthon R, Glasman P, Gombert F, Habert MO, Hampel H, Hewa H, Houot M, Jungalee N, Kas A, Kilani M, La Corte V, Le Roy F, Lehericy S, Letondor C, Levy M, Lista S, Lowrey M, Ly J, Makiese O, Masetti I, Mendes A, Metzinger C, Michon A, Mochel F, Nait Arab R, Nyasse F, Perrin C, Poirier F, Poisson C, Potier MC, Ratoehery S, Revillon M, Rojkova K, Santos-Andrade K, Schindler R, Servera MC, Seux L, Simon V, Skovronsky D, Thiebaut de Schotten M, Uspenskaya O, Vlainet M, Hovagim Bakardjian, Habib Benali, Hugo Bertin, Joel Bonheur, Laurie Boukadida, Nadia Boukerrou, Enrica Cavedo, Patrizia Chiesa, Olivier Colliot, Bruno Dubois, Marion Dubois, Stéphane Epelbaum, Geoffroy](#)

Gagliardi, Remy Genthon, Marie[HYPHEN]Odile Habert, Harald Hampel, Marion Houot, Aurélie Kas, Foudil Lamari, Marcel Levy, Simone Lista, Christiane Metzinger, Fanny Mochel, Francis Nyasse, Catherine Poisson, Marie[HYPHEN]Claude Potier, Marie Revillon, Antonio Santos, Katia Santos Andrade, Marine Sole, Mohmed Surtee, Michel Thiebaud de Schotten, Andrea Vergallo, Nadjia Younsi.

INSIGHT-preAD Scientific Committee Members: Dubois B, Hampel H, Bakardjian H, Colliot O, Habert MO, Lamari F, Mochel F, Potier MC, Thiebaut de Schotten M.

Contributors to the Alzheimer precision medicine initiative–working group (APMI–WG): Lisi Flores Aguilar (Montréal), Claudio Babiloni (Rome), Filippo Baldacci (Pisa), Norbert Benda (Bonn), Keith L. Black (Los Angeles), Arun L.W. Bokde (Dublin), Ubaldo Bonuccelli (Pisa), Karl Broich (Bonn), Francesco Cacciola (Siena), Juan Castrillo* (Derio), Enrica Cavedo (Paris), Roberto Ceravolo (Pisa), Patrizia A. Chiesa (Paris), Olivier Colliot (Paris), Jean-Christophe Corvol (Paris), Augusto Claudio Cuello (Montréal), Jeffrey L. Cummings (Las Vegas), Herman Depypere (Gent), Bruno Dubois (Paris), Andrea Duggento (Rome), Stanley Durrleman (Paris), Valentina Escott-Price (Cardiff), Howard Federoff (Irvine), Maria Teresa Ferretti (Zürich), Massimo Fiandaca (Irvine), Richard A. Frank (Malvern), Francesco Garaci (Rome), Hugo Geerts (Berwyn), Remy Genthon (Paris), Nathalie George (Paris), Filippo S. Giorgi (Pisa), Manuela Graziani (Roma), Marion Haberkamp (Bonn), Marie-Odile Habert (Paris), Harald Hampel (Paris), Karl Herholz (Manchester), Eric Karran (Cambridge), Seung H. KIM (Seoul), Yosef Koronyo (Los Angeles), Maya Koronyo-Hamaoui (Los Angeles), Foudil Lamari (Paris), Todd Langevin (Minneapolis-Saint Paul), Stéphane Lehéricy (Paris), Simone Lista (Paris), Jean Lorenceau (Paris), Dalila Mango (Rome), Mark Mapstone (Irvine), Christian Neri (Paris), Robert Nisticò (Rome), Sid E. O'Bryant (Fort Worth), Giovanni Palermo (Pisa), George Perry (San Antonio), Craig Ritchie (Edinburgh), Simone Rossi (Siena), Amira Saidi (Rome), Emiliano Santarnecchi (Siena), Lon S. Schneider (Los Angeles), Olaf Sporns (Bloomington), Nicola Toschi (Rome), Steven R. verdooner (Sacramento), Andrea Vergallo (Paris), Nicolas Villain (Paris), Lindsay A. Welikovitch (Montréal), Janet Woodcock (Silver Spring), Erfan Younesi (Esch-sur-Alzette), Mohammad Afshar (Paris), Lisi Flores Aguilar (Montréal), Leyla Akman-Anderson (Sacramento), Joaquín Arenas (Madrid), Jesus Avila (Madrid), Claudio Babiloni (Rome), Filippo Baldacci (Pisa), Richard Batrla (Rotkreuz), Norbert Benda (Bonn), Keith L. Black (Los Angeles), Arun L.W. Bokde (Dublin), Ubaldo Bonuccelli (Pisa), Karl Broich (Bonn), Francesco Cacciola (Siena), Filippo Caraci (Catania), Juan Castrillo† (Derio), Enrica Cavedo (Paris), Roberto Ceravolo (Pisa), Patrizia A. Chiesa (Paris), Jean-Christophe Corvol (Paris), Augusto Claudio Cuello (Montréal), Jeffrey L. Cummings (Las Vegas), Herman Depypere (Gent), Bruno Dubois (Paris), Andrea Duggento (Rome), Enzo Emanuele (Robbio), Valentina Escott-Price (Cardiff), Howard Federoff (Irvine), Maria Teresa Ferretti (Zürich), Massimo Fiandaca (Irvine), Richard A. Frank (Malvern), Francesco Garaci (Rome), Hugo Geerts (Berwyn), Filippo S. Giorgi (Pisa), Edward J. Goetzl (San Francisco), Manuela Graziani (Roma), Marion Haberkamp (Bonn), Marie-Odile Habert (Paris), Harald Hampel (Paris), Karl Herholz (Manchester), Felix Hernandez (Madrid), Dimitrios Kapogiannis (Baltimore), Eric Karran (Cambridge), Steven J. Kiddle (Cambridge), Seung H. Kim (Seoul), Yosef Koronyo (Los Angeles), Maya Koronyo-Hamaoui (Los Angeles), Todd Langevin (Minneapolis-Saint Paul), Stéphane Lehéricy (Paris), Alejandro Lucía (Madrid), Simone Lista (Paris), Jean Lorenceau (Paris), Dalila Mango (Rome), Mark Mapstone (Irvine), Christian Neri (Paris), Robert Nisticó (Rome), Sid E. O'Bryant (Fort Worth), Giovanni Palermo (Pisa), George Perry (San Antonio), Craig Ritchie (Edinburgh), Simone Rossi (Siena), Amira Saidi (Rome), Emiliano Santarnecchi (Siena), Lon S. Schneider (Los Angeles), Olaf Sporns (Bloomington), Nicola Toschi (Rome), Steven R. Verdooner (Sacramento), Andrea Vergallo (Paris), Nicolas Villain (Paris), Lindsay A. Welikovitch (Montréal), Janet Woodcock (Silver Spring), Erfan Younesi (Esch-sur-Alzette).^[† Deceased.]

Supplementary data

Supplementary data related to this article can be found at <https://doi.org/10.1016/j.jalz.2019.03.006>.

References

[1] H. Hampel, A. Vergallo, L.F. Aguilar, N. Benda, K. Broich, A.C. Cuello, et al., Precision pharmacology for Alzheimer's disease, *Pharmacol Res* **130**, 2018, 331–365.

[2] P.A. Chiesa, E. Cavedo, S. Lista, P.M. Thompson and H. Hampel, Revolution of resting-state functional neuroimaging genetics in Alzheimer's disease, *Trends Neurosci* **40**, 2017, 469–480.

[3] C.-C. Liu, T. Kanekiyo, H. Xu and G. Bu, Apolipoprotein E and Alzheimer disease: risk, mechanisms and therapy, *Nat Rev Neurol* **9**, 2013, 106–118.

[4] C.M. Karch and A.M. Goate, Alzheimer's disease risk genes and mechanisms of disease pathogenesis, *Biol Psychiatry* **77**, 2015, 43–51.

[5] I. Reinvang, T. Espeseth and L.T. Westlye, APOE-related biomarker profiles in non-pathological aging and early phases of Alzheimer's disease, *Neurosci Biobehav Rev* **37**, 2013, 1322–1335.

[6] C. Lane-Donovan and J. Herz, ApoE, ApoE receptors, and the synapse in Alzheimer's disease, *Trends Endocrinol Metab* **28**, 2017, 273–284.

[7] M. Fouquet, F.L. Besson, J. Gonneaud, R. La Joie and G. Chételat, Imaging brain effects of APOE4 in cognitively normal individuals across the lifespan, *Neuropsychol Rev* **24**, 2014, 290–299.

[8] P.H. Lu, P.M. Thompson, A. Leow, G.J. Lee, A. Lee, I. Yanovsky, et al., Apolipoprotein E genotype is associated with temporal and hippocampal atrophy rates in healthy elderly adults: a tensor-based morphometry study¹, *J Alzheimer's Dis* **23**, 2011, 433–442.

[9] M. Fan, B. Liu, Y. Zhou, X. Zhen, C. Xu and T. Jiang, Cortical thickness is associated with different apolipoprotein E genotypes in healthy elderly adults, *Neurosci Lett* **479**, 2010, 332–336.

[10] A.L.W. Bokde, M. Ewers and H. Hampel, Assessing neuronal networks: understanding Alzheimer's disease, *Prog Neurobiol* **89**, 2009, 125–133.

- [11] P.M. Thompson, T. Ge, D.C. Glahn, N. Jahanshad and T.E. Nichols, Genetics of the connectome, *Neuroimage* **80**, 2013, 475–488.
- [12] M.E. Raichle, The brain's default mode network, *Annu Rev Neurosci* **38**, 2015, 433–447.
- [13] Y. Chen, K. Chen, J. Zhang, X. Li, N. Shu, J. Wang, et al., Disrupted functional and structural networks in cognitively normal elderly subjects with the APOE ϵ 4 allele, *Neuropsychopharmacology* **40**, 2015, 1181–1191.
- [14] E.T. Westlye, A. Lundervold, H. Rootwelt, A.J. Lundervold and L.T. Westlye, Increased hippocampal default mode synchronization during rest in middle-aged and elderly APOE ϵ 4 carriers: relationships with memory performance, *J Neurosci* **31**, 2011, 7775–7783.
- [15] S. Matura, D. Prvulovic, M. Butz, D. Hartmann, B. Sepanski, K. Linnemann, et al., Recognition memory is associated with altered resting-state functional connectivity in people at genetic risk for Alzheimer's disease, *Eur J Neurosci* **40**, 2014, 3128–3135.
- [16] A.S. Fleisher, A. Sherzai, C. Taylor, J.B.S. Langbaum, K. Chen and R.B. Buxton, Resting-state BOLD networks versus task-associated functional MRI for distinguishing Alzheimer's disease risk groups, *Neuroimage* **47**, 2009, 1678–1690.
- [17] K.T. Patel, M.C. Stevens, G.D. Pearson, A.M. Winkler, K.A. Hawkins, P. Skudlarski, et al., Default mode network activity and white matter integrity in healthy middle-aged ApoE4 carriers, *Brain Imaging Behav* **7**, 2013, 60–67.
- [18] M.M. Machulda, Effect of APOE ϵ 4 status on intrinsic network connectivity in cognitively normal elderly subjects, *Arch Neurol* **68**, 2011, 1131.
- [19] Y.I. Sheline, J.C. Morris, A.Z. Snyder, J.L. Price, Z. Yan, G. D'Angelo, et al., APOE4 allele disrupts resting state fMRI connectivity in the absence of amyloid plaques or decreased CSF A β 42, *J Neurosci* **30**, 2010, 17035–17040.
- [20] Y. Liang, Z. Li, J. Wei, C. Li and X. Zhang, Frequency specific effects of ApoE 4 allele on resting-state networks in nondemented elders, *Biomed Res Int* **2017**, 2017, 9823501.
- [21] A.M. Staffaroni, J.A. Brown, K.B. Casaletto, F.M. Elahi, J. Deng, J. Neuhaus, et al., The longitudinal trajectory of default mode network connectivity in healthy older adults varies as a function of age and is associated with changes in episodic memory and processing speed, *J Neurosci* **38**, 2018, 2809–2817.
- [22] R.L. Buckner, Molecular, structural, and functional characterization of Alzheimer's disease: evidence for a relationship between default activity, amyloid, and memory, *J Neurosci* **25**, 2005, 7709–7717.
- [23] M. Zarei, C.F. Beckmann, M.A.A. Binnewijzend, M.M. Schoonheim, M.A. Oghabian, E.J. Sanz-Arigita, et al., Functional segmentation of the hippocampus in the healthy human brain and in Alzheimer's disease, *Neuroimage* **66**, 2013, 28–35.
- [24] H.-Y. Zhang, S.-J. Wang, J. Xing, B. Liu, Z.-L. Ma, M. Yang, et al., Detection of PCC functional connectivity characteristics in resting-state fMRI in mild Alzheimer's disease, *Behav Brain Res* **197**, 2009, 103–108.
- [25] M.D. Greicius, G. Srivastava, A.L. Reiss and V. Menon, Default-mode network activity distinguishes Alzheimer's disease from healthy aging: evidence from functional MRI, *Proc Natl Acad Sci U S A* **101**, 2004, 4637–4642.
- [26] M.I. Geerlings, C. Jonker, L.M. Bouter, H.J. Adèr and B. Schmand, Association between memory complaints and incident Alzheimer's disease in elderly people with normal baseline cognition, *Am J Psychiatry* **156**, 1999, 531–537.
- [27] B. Dubois, S. Epelbaum, F. Nyasse, H. Bakardjian, G. Gagliardi, O. Uspenskaya, et al., Cognitive and neuroimaging parameters and brain amyloidosis in individuals at risk of Alzheimer's disease (INSIGHT-preAD): a longitudinal observational study, *Lancet Neurol* **17**, 2018, 335–346.
- [28] M.G. Dik, C. Jonker, H.C. Comijs, L.M. Bouter, J.W. Twisk, G.J. van Kamp, et al., Memory complaints and APOE-epsilon4 accelerate cognitive decline in cognitively normal elderly, *Neurology* **57**, 2001, 2217–2222.
- [29] H.I.L. Jacobs, T. Hedden, A.P. Schultz, J. Sepulcre, R.D. Perea, R.E. Amariglio, et al., Structural tract alterations predict downstream tau accumulation in amyloid-positive older individuals, *Nat Neurosci* **21**, 2018, 424–431.
- [30] Y.I. Sheline, M.E. Raichle, A.Z. Snyder, J.C. Morris, D. Head, S. Wang, et al., Amyloid plaques disrupt resting state default mode network connectivity in cognitively normal elderly, *Biol Psychiatry* **67**, 2010, 584–587.
- [31] R.A. Sperling, P.S. LaViolette, K. O'Keefe, J. O'Brien, D.M. Rentz, M. Pihlajamäki, et al., Amyloid deposition is associated with impaired default network function in older persons without dementia, *Neuron* **63**, 2009, 178–188.
- [32] M.-O. Habert, H. Bertin, M. Labit, M. Diallo, S. Marie, K. Martineau, et al., Evaluation of amyloid status in a cohort of elderly individuals with memory complaints: validation of the method of quantification and determination of positivity thresholds, *Ann Nucl Med* **32**, 2018, 75–86.
- [33] F.L. Besson, R. La Joie, L. Døevre, M. Gaubert, F. Mezenge, S. Egret, et al., Cognitive and brain profiles associated with current neuroimaging biomarkers of preclinical Alzheimer's disease, *J Neurosci* **35**, 2015, 10402–10411.
- [34] C. Foulon, L. Cerliani, S. Kinkingnéhun, R. Levy, C. Rosso, M. Urbanski, et al., Advanced lesion symptom mapping analyses and implementation as BCBtoolkit, *Gigascience* **7**, 2018, 1–17.
- [35] P.N. Alves, C. Foulon, V. Karolis, D. Bzdok, D.S. Margulies, E. Volle, et al., Subcortical anatomy of the default mode network: a functional and structural connectivity study, *BioRxiv* 2019, 528679. (<https://doi.org/10.1101/528679>).

- [36] R.H.R. Pruim, M. Mennes, D. van Rooij, A. Llera, J.K. Buitelaar and C.F. Beckmann, ICA-AROMA: a robust ICA-based strategy for removing motion artifacts from fMRI data, *Neuroimage* **112**, 2015, 267–277.
- [37] G. Salimi-Khorshidi, G. Douaud, C.F. Beckmann, M.F. Glasser, L. Griffanti and S.M. Smith, Automatic denoising of functional MRI data: combining independent component analysis and hierarchical fusion of classifiers, *Neuroimage* **90**, 2014, 449–468.
- [38] J.D. Power, K.A. Barnes, A.Z. Snyder, B.L. Schlaggar and S.E. Petersen, Spurious but systematic correlations in functional connectivity MRI networks arise from subject motion, *Neuroimage* **59**, 2012, 2142–2154.
- [39] C.F. Beckmann and S.M. Smith, Probabilistic independent component analysis for functional magnetic resonance imaging, *IEEE Trans Med Imaging* **23**, 2004, 137–152.
- [40] V.D. Calhoun, T. Adali, V.B. McGinty, J.J. Pekar, T.D. Watson and G.D. Pearson, fMRI Activation in a visual-perception task: network of areas detected using the general linear model and independent components analysis, *Neuroimage* **14**, 2001, 1080–1088.
- [41] N. Filippini, B.J. MacIntosh, M.G. Hough, G.M. Goodwin, G.B. Frisoni, S.M. Smith, et al., Distinct patterns of brain activity in young carriers of the APOE-epsilon4 allele, *Proc Natl Acad Sci U S A* **106**, 2009, 7209–7214.
- [42] C.F. Beckmann, M. DeLuca, J.T. Devlin and S.M. Smith, Investigations into resting-state connectivity using independent component analysis, *Philos Trans R Soc Lond B Biol Sci* **360**, 2005, 1001–1013.
- [43] S.M. Smith, M. Jenkinson, H. Johansen-Berg, D. Rueckert, T.E. Nichols, C.E. Mackay, et al., Tract-based spatial statistics: voxelwise analysis of multi-subject diffusion data, *Neuroimage* **31**, 2006, 1487–1505.
- [44] C.D. Smith, R.J. Kryscio, F.A. Schmitt, M.A. Lovell, L.X. Blonder, W.S. Rayens, et al., Longitudinal functional alterations in asymptomatic women at risk for Alzheimer's disease, *J Neuroimaging* **15**, 2005, 271–277.
- [45] J.S. Damoiseaux, K. Prater, B.L. Miller and M.D. Greicius, Functional connectivity tracks clinical deterioration in Alzheimer's disease, *Neurobiol Aging* **33**, 2012, 1–20.
- [46] H.-Y. Zhang, S.-J. Wang, B. Liu, Z.-L. Ma, M. Yang, Z.-J. Zhang, et al., Resting brain connectivity: changes during the progress of Alzheimer Disease, *Radiology* **256**, 2010, 598–606.
- [47] W. Koch, S. Teipel, S. Mueller, K. Buerger, A.L.W. Bokde, H. Hampel, et al., Effects of aging on default mode network activity in resting state fMRI: does the method of analysis matter?, *Neuroimage* **51**, 2010, 280–287.
- [48] D.C. Park and P. Reuter-Lorenz, The adaptive brain: aging and neurocognitive scaffolding, *Annu Rev Psychol* **60**, 2009, 173–196.
- [49] G.R. Turner and R.N. Spreng, Executive functions and neurocognitive aging: dissociable patterns of brain activity, *Neurobiol Aging* **33**, 2012, 826.e1–826.e13.
- [50] M.B. Brosnan, G. Demaria, A. Petersen, P.M. Dockree, I.H. Robertson and I. Wiegand, Plasticity of the right-lateralized cognitive reserve network in ageing, *Cereb Cortex* **28**, 2018, 1749–1759.
- [51] S.W. Davis, N.A. Dennis, S.M. Daselaar, M.S. Fleck and R. Cabeza, Que PASA? The posterior-anterior shift in aging, *Cereb Cortex* **18**, 2008, 1201–1209.
- [52] S. Zhang and C.R. Li, Functional connectivity mapping of the human precuneus by resting state fMRI, *Neuroimage* **59**, 2012, 3548–3562.
- [53] D.S. Margulies, J.L. Vincent, C. Kelly, G. Lohmann, L.Q. Uddin, B.B. Biswal, et al., Precuneus shares intrinsic functional architecture in humans and monkeys, *Proc Natl Acad Sci U S A* **106**, 2009, 20069–20074.
- [54] A. Fornito, A. Zalesky and M. Breakspear, The connectomics of brain disorders, *Nat Rev Neurosci* **16**, 2015, 159–172.
- [55] R.M. Birn, K. Murphy and P.A. Bandettini, The effect of respiration variations on independent component analysis results of resting state functional connectivity, *Hum Brain Mapp* **29**, 2008, 740–750.
- [56] F. Agosta, M. Pievani, C. Geroldi, M. Copetti, G.B. Frisoni and M. Filippi, Resting state fMRI in Alzheimer's disease: beyond the default mode network, *Neurobiol Aging* **33**, 2012, 1564–1578.
- [57] X. Liu, F. Bai, C. Yue, Y. Shi, H. Yu, B. Luo, et al., The association between TOMM40 gene polymorphism and spontaneous brain activity in amnesic mild cognitive impairment, *J Neurol* **261**, 2014, 1499–1507.
- [58] N. Mattsson, R. Smith, O. Strandberg, S. Palmqvist, M. Schödl, P.S. Insel, et al., Comparing 18 F-AV-1451 with CSF t-tau and p-tau for diagnosis of Alzheimer disease, *Neurology* **90**, 2018, e388–e395.
- [59] J.A. Elman, C.M. Madison, S.L. Baker, J.W. Vogel, S.M. Marks, S. Crowley, et al., Effects of beta-amyloid on resting state functional connectivity within and between networks reflect known patterns of regional vulnerability, *Cereb Cortex* **26**, 2014, 695–707.
- [60] J.J. Palop and L. Mucke, Network abnormalities and interneuron dysfunction in Alzheimer disease, *Nat Rev Neurosci* **17**, 2016, 777–792.
- [61] A.W. Bero, P. Yan, J.H. Roh, J.R. Cirrito, F.R. Stewart, M.E. Raichle, et al., Neuronal activity regulates the regional vulnerability to amyloid- β deposition, *Nat Neurosci* **14**, 2011, 750–756.

[62] H. Hampel, K. Bürger, S.J. Teipel, A.L.W. Bokde, H. Zetterberg and K. Blennow, Core candidate neurochemical and imaging biomarkers of Alzheimer's disease, *Alzheimers Dement* **4**, 2008, 38–48.

[63] H. Hampel, S.E. O'Bryant, S. Durrleman, E. Younesi, K. Rojkova, V. Escott-Price, et al., A precision medicine initiative for Alzheimer's disease: the road ahead to biomarker-guided integrative disease modeling, *Climacteric* **20**, 2017, 107–118.

[64] M. Gold, Phase II clinical trials of anti-amyloid β antibodies: when is enough, enough?, *Alzheimers Dement Transl Res Clin Interv* **3**, 2017, 402–409.

[65] D. Prvulovic, A.L.W. Bokde, F. Faltraco and H. Hampel, Functional magnetic resonance imaging as a dynamic candidate biomarker for Alzheimer's disease, *Prog Neurobiol* **95**, 2011, 557–569.

[66] W. Koch, S. Teipel, S. Mueller, J. Benninghoff, M. Wagner, A.L.W. Bokde, et al., Diagnostic power of default mode network resting state fMRI in the detection of Alzheimer's disease, *Neurobiol Aging* **33**, 2012, 466–478.

[67] J. Gomez-Ramirez and J. Wu, Network-based biomarkers in Alzheimer's disease: review and future directions, *Front Aging Neurosci* **6**, 2014, 12.

Supplementary data

[Multimedia Component 1](#)

Supplemental Material

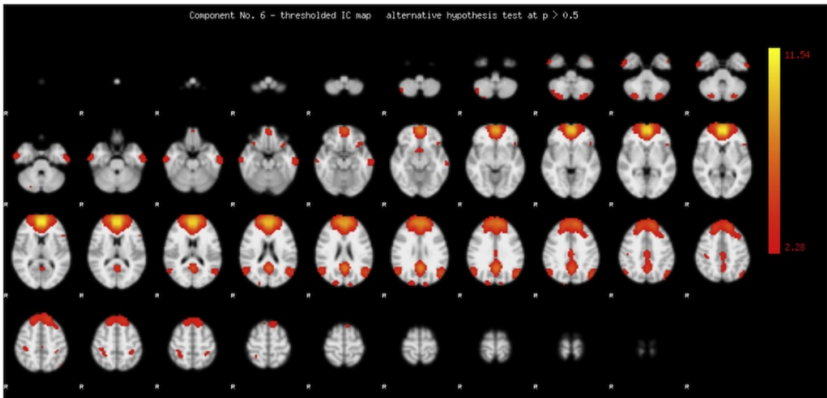


Figure S1

Highlights

- Widespread default mode network (DMN) functional connectivity changes were shown.
- *APOE* ϵ 4 [allele](#) genotype leads to distinct DMN functional alterations.
- *APOE* ϵ 4 [allele](#) leads to DMN changes regardless of the amyloid β brain deposition.

Queries and Answers

Query: If there are any drug dosages in your article, please verify them and indicate that you have done so by initialing this query

Answer: No drug dosages are included

Query: Please provide fax number for the corresponding author as it is mandatory.

Answer: Tel +33 (0)1 57 27 47 24 Fax +33 (0)1 57 27 47 24

Query: As per journal style, upto 5 keywords only allowed. Please remove any 4 keywords.

Answer: keywords: Default Mode Network; Longitudinal study; Alzheimer's disease, APOE, Amyloid β

Query: Please provide volume number for reference 35.

Answer: BioRxiv. 2019 Jan 1:528679

Query: Please provide a significance for the † symbol presented for the author “Juan Castrillo” in the Acknowledgment section.

Answer: Juan Castrillo is deceased

Query: Please verify/clarify the use of this abbreviation throughout to conform to the following: 1. “apoE” is used for the protein distinction (all roman, capital E). 2. “APOE” is used to refer to the gene (all capitals, italic). 3. If describing a diploid APOE genotype, please specify as “APOE ϵ X/ ϵ X” (where X = 2, 3, and/or 4).

Answer: OK

Query: Please note that “APOE ϵ 4 noncarriers (APOE ϵ 4+)” has been changed to “APOE ϵ 4 noncarriers (APOE ϵ 4–)” in the sentence “Participants were divided into...”. Kindly verify.

Answer: OK

Query: Please provide expansion for “PET and CATI” in the sentence “Reconstructed PET images were...”

Answer: Positron emission tomography (PET). CATI is the name of the platform (<https://cati-neuroimaging.com>)

Query: Please provide expansion for “SUVr” in the sentence “Our cohort was divided...”

Answer: Standardized uptake value ratio (SUVr)

Query: Please provide expansion for “IMAP” in the sentence “The SUVr threshold of ...”

Answer: IMAP project: Multimodal neuroimaging project on early Alzheimer's disease (Imagerie Multimodale de la maladie de l'Alzheimer a un stade Precoc)

Query: Please provide expansion for “BCB and FSL” in the sentence “The rs-fMRI data were preprocessed...”

Answer: Brain Connectivity and Behaviour (BCB) toolkit; FMRIB Software Library (FSL)

Query: Please provide expansion for “MCFLIRT” in the sentence “After individual correction for movement...”

Answer: using a motion-correction tool based on FLIRT (**MCFLIRT**)

Query: Please provide expansion for “WM and CSF” in the sentence “Estimated motion parameters, the first...”

Answer: white matter (WM) and cerebrospinal fluid (CSF)

Query: Please provide expansion for “AROMA” in the sentence “Given that rs-fMRI signal can...”

Answer: a strategy based on the independent component analysis for Automatic Removal of Motion Artifacts (ICA-AROMA) was used to...

Query: Please note that “ANOVA” has been spelled out as “analysis of variance” in the sentence “To this aim, a 2 (amyloid status...). Kindly verify. Also please provide expansion for “FEAT”.

Answer: fMRI Expert Analysis Tool (FEAT)

Query: Please provide expansion for “BA” at the first occurrence in the sentence “Second, we assessed the genetic impact...”

Answer: specifically in Brodmann area (BA) 9, BA10, BA46

Query: Please note that citation “Fig. 4” has been changed to “Fig. 3” as the text matches the caption. Also note that there are only three figures in this article.

Answer: OK

Query: Please provide expansion for “MNI” in the sentence “All results are described...”

Answer: Montreal Neurological Institute (MNI) space

Query: Please check the usage of “(A)” in figure caption 3. This is not present in artwork.

Answer: Please remove (A) from the caption 3

Query: Have we correctly interpreted the following funding source(s) and country names you cited in your article: European Research Council, European Union; AXA, France; Lilly, United States?

Answer: Yes

Query: Please provide 1st and 2nd column headings for Table 1.

Answer: No headings are required. Please consider that the first and the second column should be merged for the first two rows (participants and education).

Query: Please confirm that given names and surnames have been identified correctly and are presented in the desired order and please carefully verify the spelling of all authors' names.

Answer: Yes